emitted by the mouse remain chemically unidentified, our data suggest that they are not simple "releasers" of motor programs but that they act, at least in part, as regulators of inputs from other sensory organs. This raises two essential questions whose answers will require further insight into the function and the development of the vomeronasal pathway: (i) How is the information about the sexual identity of a conspecific processed by the brain, and how does it control animal behavior? (ii) How and when is the recognition of sex acquired by the brain, and what are the respective roles of genetic and extrinsic determinants in this developmental process?

References and Notes

1. C. J. Wysocki, *Neurosci. Biobehav.* **3**, 301 (1978).
2. A. I. Farbman, *Cell Biology of Olfaction* (Cambridge Univ. Press, New York, 1992).
3. M. Halpern, *Annu. Rev. Neurosci.* **10**, 325 (1987).
4. C. J. Wysocki, J. J. Lepri, *J. Steroid Biochem. Mol. Biol.* **39**, 661 (1991).
5. L. Buck, *Annu. Rev. Neurosci.* **19**, 517 (1995).
6. C. Dulac, R. Axel, *Cell* **83**, 195 (1995).
7. G. Herrada, D. Dulac, *Cell* **90**, 763 (1997).
8. H. Matsunami, L. Buck, *Cell* **90**, 775 (1997).
9. N. J. Ryba, R. Tirindelli, *Neuron* **19**, 371 (1997).
10. E. Pantages, C. Dulac, *Neuron* **28**, 835 (2000).
11. K. Del Punta, A. Rothman, I. Rodriguez, P. Mombaerts, *Genome Res.* **10**, 1958 (2000).
12. E. R. Liman, D. P. Corey, *J. Neurosci.* **16**, 4625 (1996).
13. ———, C. Dulac, *Proc. Natl. Acad. Sci. U.S.A.* **96**, 5791 (1999).
14. T. E. Holy, D. Dulac, M. Meister, *Science* **289**, 1569 (2000).
15. C. Dulac, *Curr. Opin. Neurobiol.* **10**, 511 (2000).
16. D. E. Clapham, L. W. Runnels, C. Strubing, *Nat. Rev. Neurosci.* **2**, 387 (2001).
17. C. Harteneck, T. D. Plant, G. Schultz, *Trends Neurosci.* **23**, 159 (2000).
18. C. S. Zuker, *Proc. Natl. Acad. Sci. U.S.A.* **93**, 571 (1996).
19. Our previous studies determined that, in the rat, rTRP2 is exclusively expressed in the microvilli of VNO sensory neurons (*13*). Recent investigation (*48*) has confirmed the expression of TRP2 in the mouse VNO, although some studies reported the presence of TRP2 transcript in testes (*21*, *22*). However, our own studies, including immunohistochemistry on tissue sections with a polyclonal antibody directed against the COOH-terminus of Trp2 (*13*), confirmed the exclusive expression of TRP2 in the VNO but failed to detect any signal in testes (*39*).
20. The following supplementary material, presented as a description, figure, or movie, is available on *Science* Online at www.sciencemag.org/cgi/content/full/1069259/DC1: supplementary fig. 1, construction of TRP2$^{-/-}$ mice; supplementary fig. 2, VNO receptor survival in TRP2$^{+/-}$ and TRP2$^{-/-}$ mice; supplementary materials and methods for construction of TRP2$^{-/-}$ mice, Western blot analysis, electrophysiology, electrophysiology data analysis, in situ and histological analysis, mating behavior, male-male aggression, testosterone RIA analysis, and ultrasonic vocalization analysis.
21. M. K. Jungnickel, H. Marrero, L. Birnbaumer, J. R. Lemos, H. M. Florman, *Nature Cell Biol.* **3**, 499 (2001).
22. B. Vannier *et al.*, *Proc. Natl. Acad. Sci. U.S.A.* **93**, 571 (1996).
23. X. Z. Xu, F. Chien, A. Butler, L. Salkoff, C. Montell, *Neuron* **26**, 647 (2000).
24. H. S. Li, C. Montell, *J. Cell Biol.* **150**, 1411 (2000).
25. L. Belluscio, G. Koentges, R. Axel, C. Dulac, *Cell* **97**, 209 (1999).
26. D. Lin et al., *Neuron* **26**, 69 (2000).
27. C. Zheng, P. Feinstein, T. Bozza, I. Rodriquez, P. Mombaerts, *Neuron* **26**, 31 (2000).
28. H. Zhao, R. R. Reed, *Cell* **104**, 651 (2001).
29. M. Meredith, *Physiol. Behav.* **36**, 737 (1986).
30. J. B. Powers, S. S. Winans, *Physiol. Behav.* **10**, 361 (1973).
31. D. A. Edwards, K. G. Burge, *Physiol. Behav.* **11**, 867 (1973).
32. A. N. Clancy, A. Coqulin, F. Macrides, R. A. Gorski, E. P. Noble, *J. Neurosci.* **4**, 2222 (1984).
33. N. J. Bean, *Physiol. Behav.* **29**, 433 (1982).
34. J. Connor, *Psychon. Sci.* **27**, 1 (1972).
35. J. A. Maruniak, C. J. Wysocki, J. A. Taylor, *Physiol. Behav.* **37**, 655 (1986).
36. P. M. Driver, D. A. Humphries, *Nature* **226**, 967 (1970).
37. M. S. Barkley, B. D. Goldman, *Horm. Behav.* **9**, 32 (1977).
38. C. T. Lee, S. C. Brake, *Psychon. Sci.* **27**, 287 (1972).
39. L. Stowers, C. Dulac, data not shown.
40. M. L. Sipos, C. J. Wysocki, J. G. Nyby, L. Wysocki, T. A. Nemura, *Physiol Behav.* **58**, 529 (1995).
41. J. R. Alberts, B. G. Galef Jr., *Physiol Behav.* **6**, 619 (1971).
42. G. A. Van Oortmerssen, *Behaviour* **38**, 1 (1971).
43. J. Nyby, C. J. Wysocki, G. Whitney, G. Dizinno, J. Schneider, *J. Comp. Physiol. Psychol.* **93**, 957 (1979).
44. R. A. Zann, *The Zebra Finch: A Synthesis of Field and Laboratory Studies* (Oxford Univ. Press, Oxford, 1996).
45. E. Keverne, *Science* **286**, 716 (1999).
46. M. Meredith, *Chem. Senses* **26**, 433 (2001).
47. J. Nathans, *Neuron* **24**, 299 (1999).
48. T. Hofmann, M. Schaefer, G. Schultz, T. Gudermann, *Biochem J.* **351**, 115 (2000).
49. We thank M. A. Wilson for experimental advice; R. Hellmiss-Peralta for the illustration; T. C. Lee for help with the manuscript preparation; P. Jiang, J. Dubauskaite, and M. E. Klein for help with gene targeting; and D. Haig and members of the Dulac and Meister labs for helpful comments. Financially supported by the Howard Hughes Medical Institute (L.S.); NIH grant DC03903 (C.D.); and Office of Naval Research grant (M.M.), Human Frontier Science Program (G.K.), and Jane Coffin Childs Memorial Fund (T.E.H.) fellowships.

21 December 2001; accepted 23 January 2002
Published online 31 January 2002;
10.1126/science.1069259
Include this information when citing this paper.

A Rational Chemical Synthesis of C_{60}

**Lawrence T. Scott,[1]* Margaret M. Boorum,[1]
Brandon J. McMahon,[1] Stefan Hagen,[1] James Mack,[1]
Jarred Blank,[1] Hermann Wegner,[1,2] Armin de Meijere[2]**

Isolable quantities of C_{60}, the smallest stable fullerene, have been synthesized in 12 steps from commercially available starting materials by rational chemical methods. A molecular polycyclic aromatic precursor bearing chlorine substituents at key positions forms C_{60} when subjected to flash vacuum pyrolysis at 1100°C. No other fullerenes are formed as by-products. The methods we have developed for the target-specific synthesis of fullerenes, applied here to a synthesis of C_{60}, should make possible the directed laboratory preparation of other fullerenes as well, including those not accessible by graphite vaporization.

Although C_{60} and some of the higher fullerenes can be readily prepared by resistive heating of graphite (*1*), there is still considerable interest in the rational stepwise synthesis of these geodesic all-carbon compounds in isolable quantities. Such approaches may allow derivatives of fullerenes to be prepared and may also provide access to fullerenes that are not obtained through the uncontrolled vaporization of graphite.

We recently showed that hydrocarbon **1**, which incorporates all 60 carbon atoms, 13 of the 20 benzene rings, and 75 of the 90 carbon-carbon bonds required to form C_{60}, can be "stitched up" with a high-energy laser to generate C_{60} (Fig. 1) (*2*). That method, however, did not permit isolation of the fullerene produced. We have therefore drawn on our experience with the synthesis of smaller geodesic polyarenes, which taught us that incorporation of halogen atoms at strategic sites on polycyclic aromatic hydrocarbons invariably improves the preparative yields of such high-energy reactions, often by two orders of magnitude or more (*3*–*5*). We now report that preparative-scale flash vacuum pyrolysis (FVP) of the chlorinated hydrocarbon **2** at 1100°C (*6*, *7*) does, in fact, induce the desired carbon-carbon bond-forming reactions, stitching together the arms of the molecular precursor according to plan and forming the all-carbon polyhedron (Fig. 1). No C_{70} or any other fullerenes would be expected from such a process, and none are detected in the syn-

---

[1] Department of Chemistry, Merkert Chemistry Center, Boston College, Chestnut Hill, MA 02467–3860, USA. [2] Institut für Organische Chemie der Georg-August-Universität, Tammannstrasse 2, D-37077 Göttingen, Germany.

*To whom correspondence should be addressed. E-mail: lawrence.scott@bc.edu

thetic material; C_{60} is the only fullerene formed.

Figure 2 summarizes the route we devised to synthesize compound **2** (*8*), using classical organic chemistry and a straightforward adaptation of our earlier route to the parent $C_{60}H_{30}$ hydrocarbon (*2*). New carbon-carbon bonds are formed by a Grignard addition (step a), a Wittig reaction (step d), a stilbene photocyclization (step e), an S_N2 displacement (step g), a Friedel-Crafts cyclization (step j), and an aldol cyclotrimerization (step k). For the photocyclization step, the alkene *E* and *Z* isomers obtained as a mixture from step d could be used without separation, because they interconvert photochemically. For the pyrolysis (Fig. 1), it would have been preferable to have the chlorine atoms located at the mouths of the fjord regions (sites marked by asterisks in Fig. 1), but we found that the extra steric strain this imposes on the molecule adversely affects the yield of the aldol cyclotrimerization (*9*). Fortunately, the mobility of hydrogen atoms in aryl radicals at high temperatures (*10*, *11*) allowed us the freedom to incorporate the chlorine atoms one position removed from the mouth of each fjord region.

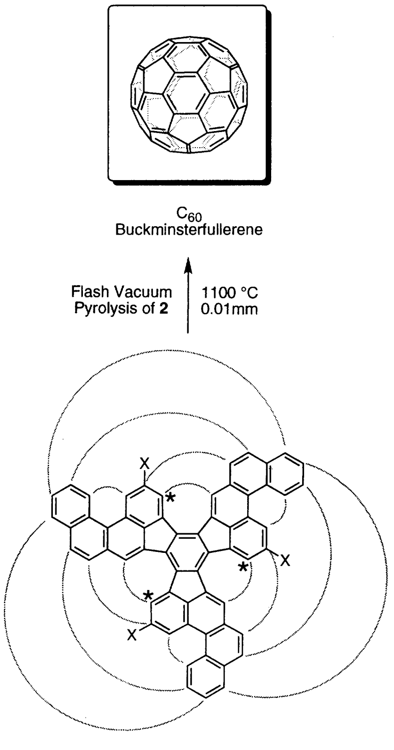

1 X = H　　**2** X = Cl

Fig. 1. Final step in the synthesis of C_{60}. Curved lines indicate where the new bonds are formed in the molecular precursor **2** ($C_{60}H_{27}Cl_3$). The fjord regions mentioned in the text are marked with asterisks. We have previously generated C_{60} in a mass spectrometer by laser-induced cyclodehydrogenation of the corresponding hydrocarbon, **1** (*2*).

Mass spectrometric analysis provided positive identification of C_{60} in the product mixture obtained from the final step of the synthesis. To ensure that the C_{60} we detected really came from the synthesis and was not being formed during the mass spectrometric analysis, we relied on the relatively gentle technique of electrospray mass spectrometry (ES-MS). This is a critical point, given that the more energetic technique of laser desorption ionization mass spectrometry transforms even the parent hydrocarbon **1** into C_{60} inside a mass spectrometer (*2*).

A good protocol for the detection of fullerenes by ES-MS, run in negative ion mode, involves pretreatment of the fullerenes with zinc powder in a mixture of tetrahydrofuran and aqueous sodium hydroxide under a nitrogen atmosphere (*12*). Under these conditions, fullerenes are easily reduced to their monoanion radicals, which are stable in the absence of oxygen and acid; most polycyclic aromatic hydrocarbons and their derivatives, however, remain neutral. When a portion of our unpurified synthetic material is treated with zinc in this manner and then analyzed by ES-MS, a prominent peak for C_{60} is seen at a mass-to-charge ratio (*m/z*) of 720 (Fig. 3A).

No peaks were detected for C_{70} or for any other fullerenes in the mass spectrum of the synthetic material. Control experiments in our laboratory with the zinc reduction protocol and a C_{60}/C_{70} fullerene mixture purchased from a commercial source gave mass spectral peaks not only for both C_{60} and C_{70} (*m/z* 720 and 840, respectively) but also for C_{78} and C_{84} (*m/z* 936 and 1008, respectively), which were apparently present in the sample as minor impurities. The great sensitivity of this analytical method establishes that C_{60} is the exclusive fullerene formed in the laboratory synthesis reported here.

As independent confirmation that C_{60} is produced in the final step of the synthesis, a high-pressure liquid chromatographic (HPLC) analysis was performed. Using conditions under which authentic C_{60} elutes in 4.64 min (*13*), we found that the synthetic material also gives an HPLC peak at 4.64 min (Fig. 4). Furthermore, the synthetic product that matches the retention time of authentic C_{60} gives a diode array ultraviolet-visible (UV-VIS) absorption spectrum that matches the spectrum of authentic C_{60} (Fig. 5).

Finally, a portion of the crude product from the synthesis was subjected to HPLC, and the fullerene fractions from multiple injections were collected (*14*). The isolated fullerene fractions were then combined, concentrated to dryness, dissolved in *ortho*-dichlorobenzene, and treated with sodium cyanide and dimethylformamide under a nitrogen atmosphere, according to the procedure of Komatsu *et al.* (*15*). Under these conditions, authentic C_{60} is rapidly converted to $[C_{60}(CN)]^-$, which can be seen at *m/z* 746 by ES-MS in negative ion mode. An ES-MS analysis of the material isolated from the synthetic product mixture by HPLC and treated with sodium cyanide likewise shows an

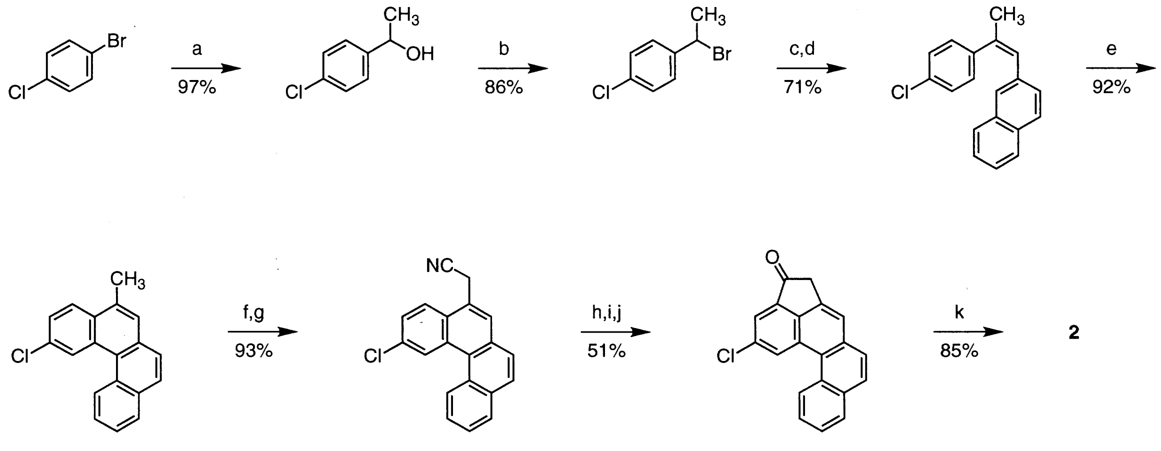

Fig. 2. Synthesis of the C_{60} precursor **2** ($C_{60}H_{27}Cl_3$). Step a: Treatment with Mg in ether, then acetaldehyde. b: Bromination with PBr_3 in benzene. c: Treatment with $P(C_6H_5)_3$ in toluene. d: Treatment with $LiOCH_2CH_3$ and 2-naphthaldehyde in ethanol/dichloromethane. e: Irradiation with UV light (254 nm) in cyclohexane containing iodine and propylene oxide. f: Bromination with *N*-bromosuccinimide and dibenzoylperoxide in carbon tetrachloride. g: Displacement with KCN and tetrabutylammonium hydrogensulfate in water/dichloromethane. h: Hydrolysis with KOH in ethylene glycol. i: Chlorination with $SOCl_2$. j: Cyclization with $AlCl_3$ in dichloromethane. k: Trimerization with $TiCl_4$ in *ortho*-dichlorobenzene.

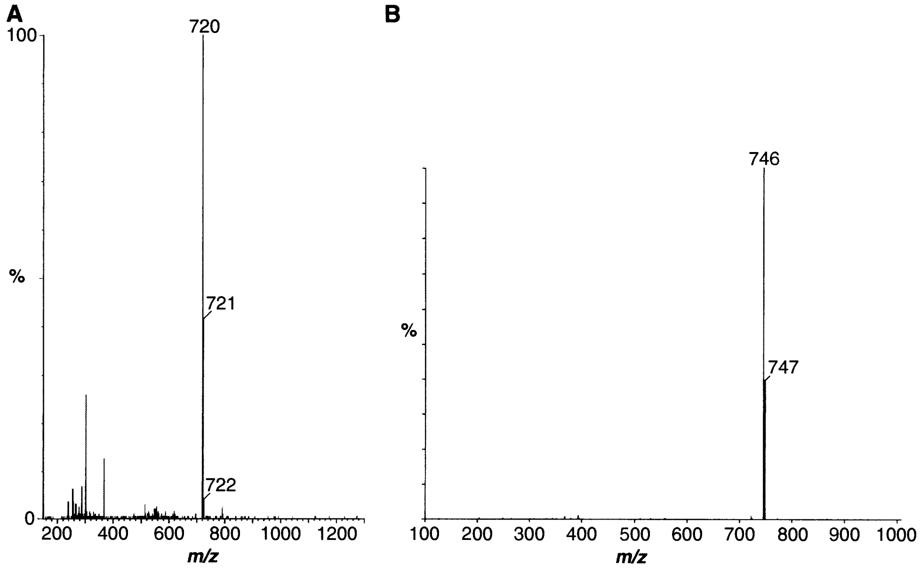

Fig. 3. (**A**) Electrospray mass spectrum, run in negative ion mode, of the unpurified product from the reaction in Fig. 1, after reduction with zinc. The molecular ion of C_{60} gives the base peak at *m/z* 720. No signals were detected for C_{70} or for any higher fullerenes. The peaks at *m/z* 721 and 722 reflect the 1.1% natural abundance of the ^{13}C isotope in our synthetic C_{60}. (**B**) Electrospray mass spectrum of $[C_{60}(CN)]^-$ (*m/z* 746) obtained by adding sodium cyanide (*15*) to the C_{60} that was synthesized as in Fig. 1 and isolated by HPLC. No peaks corresponding to the known cyanide adducts of C_{70} or of any higher fullerenes were detected.

Fig. 4. HPLC analysis of the product obtained from the reaction in Fig. 1. The peak at 4.64 min appears at the same retention time as the peak given by authentic C_{60}. The identities of the other products that elute faster than C_{60} have not yet been determined. abs., absorbance.

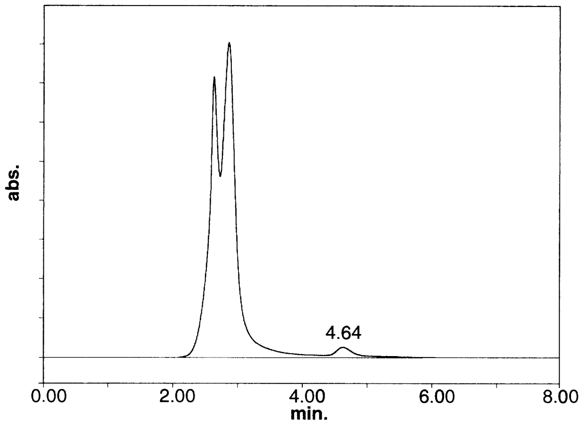

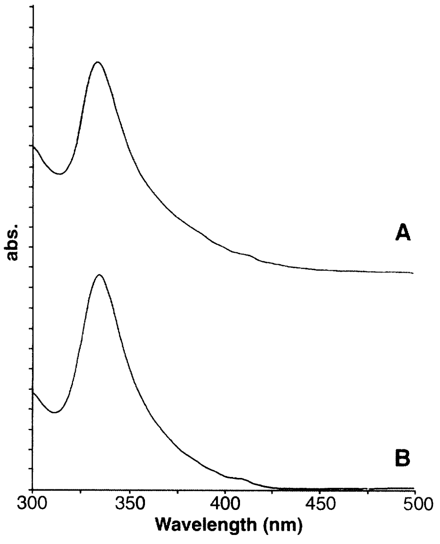

Fig. 5. Diode array UV-VIS absorption spectra of the HPLC peak at 4.64 min (55:45 toluene: acetonitrile) from authentic C_{60} (**A**) and from the product obtained from the reaction in Fig. 1 (**B**).

m/z 746 peak for $[C_{60}(CN)]^-$ (Fig. 3B). No peaks corresponding to the known cyanide adducts of C_{70} or of any higher fullerenes could be detected. Again, the evidence indicates that C_{60} is formed exclusive of all other fullerenes.

Previous attempts to synthesize C_{60} from molecular precursors have resulted, at best, only in the generation of gas-phase C_{60} under high-energy conditions in a mass spectrometer (*2*, *16–20*).

The overall yield of our 12-step synthesis in its current state of development is not high; however, the pyrolysis precursor **2** is accessible on a multigram scale. The amount of C_{60} produced in the final step can presently be estimated only qualitatively from the size of the C_{60} peak in the HPLC analysis (~3% relative area, Fig. 4) and the material balance (20 to 27% mass recovery from three independent runs), which leads to an estimated yield in the range of 0.1 to 1.0%. From a practical viewpoint, this synthesis will not supplant graphite vaporization as a cheap source of C_{60}, but that was not our goal.

How "rational" is a synthesis that relies on FVP as the method for closing up the fullerene ball? Our design of compound **2** as a molecular precursor to C_{60} was guided by four key principles, all of which have come to light just in the past 10 years, primarily from work in our laboratory. First, FVP has emerged as a powerful method for providing the energy required to transform planar polycyclic aromatic hydrocarbon ring systems into their strained geodesic counterparts. This strategy was used in our synthesis of corannulene (*21*, *22*) and has subsequently enabled syntheses of many other open geodesic polyarenes (*3*, *23*). Second, for the imposition of curvature on a planar, polycyclic π system by FVP, cyclization reactions initiated by specifically generated aryl radicals are invariably superior, often by two orders of magnitude or more in yield, to those based on undirected thermal cyclodehydrogenations (*3–5*). Third, the ability of aryl radicals to rearrange by 1,2 shifts of hydrogen atoms under FVP conditions (*10*) gives one the latitude to incorporate radical precursors (such as halogen atoms) at sites dictated by synthetic expedience rather than just at those sites where the initial cyclizations must occur (*11*). Finally, once curvature has been locked in, cyclodehydrogenation reactions become more favorable for subsequent ring closures (*24*, *25*).

The absence of C_{70} and higher fullerenes in our synthetic material can be taken as good evidence that precursor **2** does indeed "zip up" intramolecularly to C_{60}, as illustrated in Fig. 1. Such intramolecular aryl-aryl coupling reactions are now abundantly precedented and have found considerable use in recent years for the directed synthesis of simpler geodesic polyarenes from planar precursors that have the same number of carbon atoms but lack two or more carbon-carbon bonds (*3*, *23*). A mechanism for C_{60} formation involving decomposition of **2** to small pieces that recombine, as in the vaporization of graphite (*26*), would be expected to give C_{70} and higher fullerenes as well.

References and Notes

1. W. Krätschmer, L. D. Lamb, K. Fostiropoulos, D. R. Huffman, *Nature* **347**, 354 (1990).
2. M. M. Boorum, Y. V. Vasil'ev, T. Drewello, L. T. Scott, *Science* **294**, 828 (2001).

3. L. T. Scott, *Pure Appl. Chem.* **68**, 291 (1996) and references cited therein.
4. L. T. Scott, M. S. Bratcher, S. Hagen, *J. Am. Chem. Soc.* **118**, 8743 (1996).
5. R. B. M. Ansems, L. T. Scott, *J. Am. Chem. Soc.* **122**, 2719 (2000).
6. Pyrolyses of **2** were carried out at an oven temperature of 1100°C as described previously for other substrates (*4*, *7*), with a steady stream of nitrogen carrier gas flowing through the sample chamber from a thin capillary connected to a 1-atm reservoir (final pressure with the nitrogen flowing = ~0.01 mm Hg). To promote sublimation of **2**, the sample chamber was heated to 350°C for 45 min and then to 400°C for an additional 60 min. Pyrolysis of a 120-mg sample of **2** at 1100°C, using an unpacked quartz tube, gave 27 mg of crude product in the pyrolysis trap. Filling the pyrolysis tube with quartz rings resulted in a lower material balance and a poorer conversion to C_{60}.
7. A. Necula, L. T. Scott, *J. Anal. Appl. Pyrol.* **54**, 65 (2000).
8. The first 10 reactions summarized in Fig. 2 (steps a through j) were run under essentially standard conditions, and the products were thoroughly characterized by combustion analysis and/or high-resolution mass spectroscopy, ^{1}H nuclear magnetic resonance (NMR), ^{13}C NMR, and, where appropriate, infrared spectroscopy (*9*). The final step (k) was run on a 641-mg scale in 25 ml of *ortho*-dichlorobenzene with 2.4 molar equivalents of $TiCl_4$ at 100°C for 130 min, under conditions similar to those that have proven successful for numerous other aldol trimerizations of related systems in our laboratory (*5*, *9*, *24*). The product (**2**) gave a base peak for the molecular ion in the matrix-assisted laser desorption-ionization (MALDI) mass spectrum (calculated for $C_{60}H_{27}Cl_3$, 852.1178; found, 852.1138), but it is too insoluble to permit complete characterization by ^{1}H NMR spectroscopy. The only significant byproduct in the $TiCl_4$ reaction was the next higher homolog of **2**, the cyclic tetramer (MALDI mass spectrum: calculated for $C_{80}H_{36}Cl_4$, 1136.1571; found, 1136.1540).
9. M. M. Boorum, thesis, Boston College, Chestnut Hill, MA (2001).
10. M. A. Brooks, L. T. Scott, *J. Am. Chem. Soc.* **121**, 5444 (1999).
11. S. Hagen, M. S. Bratcher, M. S. Erickson, G. Zimmermann, L. T. Scott, *Angew. Chem. Int. Ed. Engl.* **36**, 406 (1997).
12. M. Wu, X. Wei, L. Qi, Z. Xu, *Tetrahedron Lett.* **37**, 7409 (1996).
13. For analytical purposes, the product mixtures from the pyrolyses were chromatographed on a Kontron ODS2 Techsphere 5 column (no. 421CTS-155125, with fully end-capped octadecylsilane-covered spherical silica, measuring 125 mm by 4.6 mm, and containing 5-μm particles), monitoring at 335 nm with a diode array UV-VIS detector, and eluting with 55:45 toluene:acetonitrile (0.5 ml/min).
14. For the isolation of C_{60}, a Supelco SUPELCOSIL LC-PAH ODS column (250 mm by 4.6 mm, containing 5-μm particles) was used with UV monitoring at 335 nm and 1:1 toluene:acetonitrile as the eluant (1.2 ml/min). Collection of the effluent from the column commenced ~1 min before the C_{60} peak appeared in the chromatogram and continued for a period of at least 5 min for each run. When a mixture of authentic C_{60} and C_{70} is chromatographed and collected in this manner, both fullerenes are detected in the mass spectroscopic analysis. The product mixture from the pyrolysis, on the other hand, gives only C_{60} and no C_{70}.
15. K. Komatsu, K. Fujiwara, Y. Murata, *Chem. Commun.* **2000**, 1583 (2000).
16. Y. Rubin, M. Kahr, C. B. Knobler, F. Diederich, C. L. Wilkins, *J. Am. Chem. Soc.* **113**, 495 (1991).
17. S. W. McElvany, M. M. Ross, N. S. Goroff, F. Diederich, *Science* **259**, 1594 (1993).
18. Y. Rubin *et al.*, *Angew. Chem. Int. Ed. Engl.* **37**, 1226 (1998).
19. Y. Tobe *et al.*, *J. Am. Chem. Soc.* **120**, 4544 (1998).
20. Y. Tobe *et al.*, *Tetrahedron* **57**, 3629 (2001).
21. L. T. Scott, M. M. Hashemi, D. T. Meyer, H. B. Warren, *J. Am. Chem. Soc.* **113**, 7082 (1991).
22. L. T. Scott *et al.*, *J. Am. Chem. Soc.* **119**, 10963 (1997).
23. L. T. Scott *et al.*, *Pure Appl. Chem.* **71**, 209 (1999) and references cited therein.
24. B. J. McMahon, thesis, Boston College, Chestnut Hill, MA (1997).
25. M. D. Clayton, P. W. Rabideau, *Tetrahedron Lett.* **38**, 741 (1997).
26. N. S. Goroff, *Acc. Chem. Res.* **29**, 77 (1996).
27. Financial support for this work was generously provided by NSF and the U.S. Department of Energy. Fellowships for L.T.S., S.H., and H.W. from the Alexander von Humboldt Foundation, the German Academic Exchange Service, and the Fulbright Foundation, respectively, are also gratefully acknowledged. High-resolution mass spectra were recorded at the University of Illinois, Urbana-Champaign, and the University of California, Riverside.

27 November 2001; accepted 18 January 2002

Array-Based Electrical Detection of DNA with Nanoparticle Probes

So-Jung Park, T. Andrew Taton,* Chad A. Mirkin†

A DNA array detection method is reported in which the binding of oligonucleotides functionalized with gold nanoparticles leads to conductivity changes associated with target-probe binding events. The binding events localize gold nanoparticles in an electrode gap; silver deposition facilitated by these nanoparticles bridges the gap and leads to readily measurable conductivity changes. An unusual salt concentration–dependent hybridization behavior associated with these nanoparticle probes was exploited to achieve selectivity without a thermal-stringency wash. Using this method, we have detected target DNA at concentrations as low as 500 femtomolar with a point mutation selectivity factor of ~ 100,000:1.

A major challenge in the area of DNA detection (*1*) is the development of methods that do not rely on polymerase chain reaction (PCR) or comparable target-amplification systems that require additional instrumentation and reagents that are not ideal for point-of-care or field use. Another restrictive requirement of most DNA detection systems, regardless of their need for PCR, is a thermal-stringency wash to differentiate target strands from ones with mismatches and thus achieve desired analyte selectivity. We previously reported several optical DNA detection methods based on oligonucleotide-modified Au nanoparticles and their size-dependent scattering, catalytic, and absorption properties (*2*–*5*). We also showed that Au particles that are heavily functionalized with oligonucleotides exhibit extraordinarily sharp thermal-denaturation profiles that translate into higher target selectivities (*2*–*5*). We now report a conductivity-based DNA detection method utilizing oligonucleotide-functionalized Au nanoparticles that provides an alternative to existing detection methods (*6*–*11*) and presents a straightforward approach to high-sensitivity and -selectivity, multiplexed detection of DNA.

In the detection scheme (Fig. 1A), selective binding occurs between a shorter "capture" oligonucleotide strand located in the gap between two fixed microelectrodes and a longer "target" oligonucleotide in solution. The target oligonucleotide has contiguous recognition elements that are complementary to the capture strand on one end and on the other to oligonucleotides attached to Au nanoparticles (Fig. 1B). Therefore, when the device with the pair of electrodes is immersed in a solution containing the appropriate probe and target, Au nanoparticle probes fill the gap.

In principle, capacitance or conductivity measurements can be made to determine the number of particles and, therefore, target molecules that fill the gap. However, the sensitivity of the device can be markedly increased by exposing the active component of the device to a solution of Ag(I) and hydroquinone (photographic developing solution). The use of Au nanoparticles as promoters for Ag(I) reduction has been exploited in colorimetric detection schemes for DNA and proteins (*4*, *12*). Moreover, we and others have evaluated the electrical properties of DNA-modified nanoparticles, protein-modified nanoparticles, aggregates, and structures formed from Ag reduction on individual particles (*13*–*15*), and those data suggest that the system described in Fig. 1A should be viable, provided that enough particles can fill the gaps and give a measurable electrical signal.

Such a strategy can be extended to arrays (*16*), where each component of the array is an

---

Department of Chemistry and Institute for Nanotechnology, Northwestern University, Evanston, IL 60208, USA.

*Present address: Department of Chemistry, University of Minnesota, Minneapolis, MN 55455, USA.

†To whom correspondence should be addressed. E-mail: camirkin@chem.northwestern.edu